PHYSICAL REVIEW B **78**, 024521 (2008)

Intrinsic properties of stoichiometric LaFePO

T. M. McQueen,[1] M. Regulacio,[1] A. J. Williams,[1] Q. Huang,[2] J. W. Lynn,[2] Y. S. Hor,[1] D. V. West,[1] M. A. Green,[2,3] and R. J. Cava[1]

[1]*Department of Chemistry, Princeton University, Princeton, New Jersey 08544, USA*

[2]*NIST Center for Neutron Research, National Institute of Standards and Technology, Gaithersburg, Maryland 20899, USA*

[3]*Department of Materials Science and Engineering, University of Maryland, College Park, Maryland 20742-2115, USA*

(Received 14 May 2008; published 29 July 2008)

DC and ac magnetization, resistivity, specific-heat, and neutron-diffraction data reveal that stoichiometric LaFePO is metallic and non-superconducting above $T=0.35$ K, with $\gamma=12.5\frac{\text{mJ}}{\text{mol K}^2}$. Neutron-diffraction data at room temperature and $T=10$ K are well described by the stoichiometric, tetragonal ZrCuSiAs structure, and show no signs of structural distortions or long-range magnetic ordering to an estimated detectability limit of $0.07\mu_B$/Fe. We propose a model based on the shape of the iron-pnictide tetrahedron that explains the differences between LaFePO and LaFeAsO, the parent compound of the recently discovered high-Tc oxyarsenides, which, in contrast, shows both structural and spin-density wave transitions.

DOI: 10.1103/PhysRevB.78.024521 PACS number(s): 74.70.Dd, 74.25.Bt, 61.05.fm

I. INTRODUCTION

The compounds LnFeXO (Ln=La…Gd, X=P, As) were first synthesized in 1995 (X=P) (Ref. 1) and 2000 (X=As) (Ref. 2). However, it was not until 2006 that the first report of superconductivity in this class of compounds, in LaFePO, was published.[3] Since then, a range of transition temperatures have been reported in fluorine doped ($LnFeXO_{1-x}F_x$) and oxygen deficient ($LnFeXO_{1-x}$) variants, including T_c that are greater than $T=50$ K in $SmFeAsO_{1-x}F_x$.[4–27] Thus this class of superconductors has the highest transition temperatures known except for the cuprates. The origin of the remarkably high T_c has been the subject of considerable debate. One interesting observation is that while LaFeAsO is metallic but nonsuperconducting,[28] LaFePO has been reported as a superconductor.[3,29,30] The reported T_c in LaFePO have varied from $T=3.1$ K (Ref. 3) to 7 K (Ref. 30), and appear to depend on the sample form and synthesis conditions.[29,31,32] However, to date there has been no complete study of LaFePO. In particular, neither resistivity nor susceptibility measurements (used in the above cited works on LaFePO) are conclusive proof of bulk superconductivity as both can be sensitive to impurities. Instead, the presence or absence of an anomaly in the specific heat is a more reliable indicator of bulk properties, including superconductivity. The original aim of our work was to investigate the superconductivity in pure LaFePO. Instead we have found that, through an exhaustive set of measurements, stoichiometric LaFePO is not a superconductor above $T=0.35$ K. Additionally, we find that it is a metal with no long-range magnetic ordering or structural distortions above $T=10$ K. These properties make LaFePO closer to LaFeAsO than previously thought. We also provide a chemical explanation for the difference in the behavior of LaFePO compared to LaFeAsO.

II. EXPERIMENT

Polycrystalline samples of LaFePO were synthesized in multiple steps. First, LaP was synthesized by reacting fresh La shavings and dry P powder in an alumina crucible in a sealed, evacuated silica ampoule; the ampoule was immediately heated to 400 °C then ramped at 20 °C/h to 800 °C. The temperature was held for 20 h and then the sample was furnace cooled. Next, a stoichiometric ~2.5 g mixture of LaP, Fe, and Fe_3O_4 was ground together and pressed into a pellet. This pellet was placed with 5% excess P in an alumina crucible with a tight-fitting alumina cap. This crucible was placed on quartz shards inside a quartz tube. A second, smaller, alumina crucible containing ~80 mg of impure LaFePO from a previous run was also placed in the quartz tube, which was then pumped down and sealed under vacuum. The sample was ramped to 1200 °C at 180 °C/h, held at temperature for 48 h, and then cooled at 180 °C/h to room temperature. After that the sample was removed, reground, repressed, and heated with an additional 5% excess P as before. This was repeated a third time to achieve phase purity. In each repetition, the pellets of LaFePO came out clean with no visible undesired reactivity even on the surface. The alumina crucibles and quartz tubes were also clean and undamaged. In contrast, the impure LaFePO getterer on top came out visibly different in color; x-ray diffraction confirmed the presence of silicate formation. In further processing, the material was protected from air as it was found to decompose with extended exposure to moisture.

DC magnetization measurements between $T=1.8$ K and $T=300$ K were performed on a quantum design magnetic property measurement system (MPMS) magnetometer with applied fields of $\mu_0 H=0.0005$ and 1 T. AC magnetization measurements were performed on a quantum design physical property measurement system (PPMS) with a dc field of $\mu_0 H_{dc}=0.0005$ T and an ac field of $\mu_0 H_{ac}=0.0003$ T at $f=1$ kHz. Resistivity and specific-heat measurements were done on polycrystalline pellets between $T=0.35$ and 300 K in a quantum design PPMS equipped with a ^{3}He refrigerator. Thermopower measurements were done using a custom-built helium probe-head and MMR technologies electronics.

High resolution neutron powder-diffraction (NPD) data were collected using the BT-1 high-resolution powder diffractometer at the NIST Center for Neutron Research, employing Cu (311) monochromator to produce a monochro-

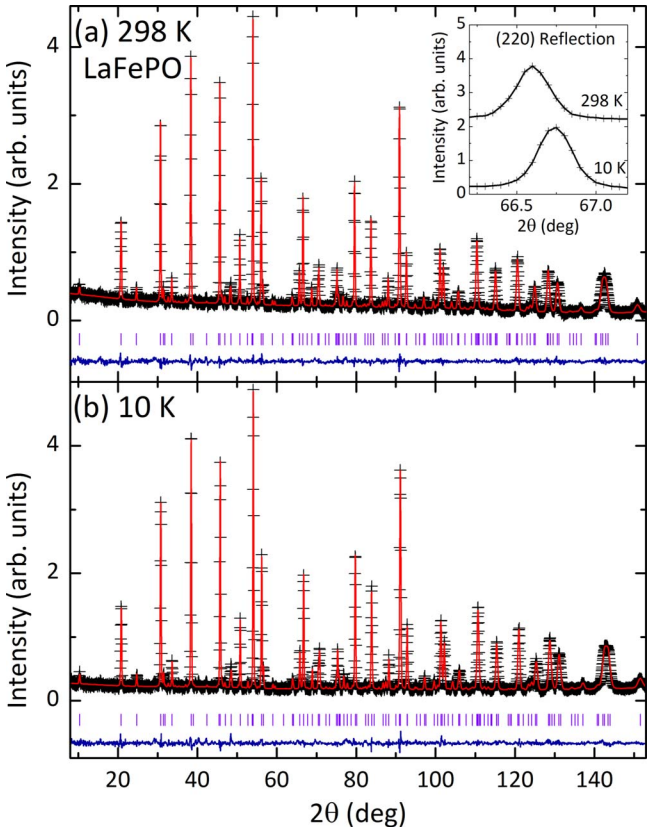

FIG. 1. (Color online) Neutron powder-diffraction data with Rietveld fits at (a) 298 and (b) 10 K. The tick marks correspond to LaFePO. The inset of (a) shows the lack of splitting in the (220) reflection on cooling.

matic neutron beam of wavelength 1.5403 Å. Collimators with horizontal divergences of 15′, 20′, and 7′ full width at half maximum were used before and after the monochromator, and after the sample, respectively. The intensities were measured in steps of 0.05 ° in the 2θ range 3 °–168 °. The structure analysis was performed using the program GSAS with EXPGUI.[33,34] The neutron-scattering amplitudes used in the refinements were 0.827, 0.954, 0.581, and 0.513 ($\times 10^{-12}$ cm) for La, Fe, O, and P, respectively. To investigate possible magnetic ordering, additional data were collected on the high intensity/coarse resolution BT-7 spectrometer with a pyrolytic graphite monochromator and filter using a wavelength of 2.44 Å, and a position sensitive detector in diffraction mode.

III. RESULTS

Figure 1 shows neutron powder-diffraction patterns collected at room temperature and $T=10$ K along with the fits from Rietveld refinements. The patterns are well described by the tetragonal phase LaFePO and this structure is shown in Fig. 2(a). It consists of P-Fe_2-P layers of edge-sharing Fe-P tetrahedra separated by La-O_2-La-type sheets. The iron ions form two-dimensional square nets where the Fe-Fe distance is 2.80 Å at room temperature. Table I summarizes the results from the structure fits. Since previous results in the As case suggest that fluorine doping or oxygen nonstoichiometry induce superconductivity, we allowed the occupancies of the La, O, and P sites to vary in the $T=298$ K refinement. Within error, all occupancies are equal to one (column 1, Table I). As a further test of the stoichiometry, the thermal parameters were held fixed and all four occupancies were refined (column 2, Table I). Again, within error all occupancies are equal to one and thus were fixed at unity for the final refinements (columns 3 and 4, Table I). The quality of the fits is excellent. We included minor impurity phases of 0.6% La_2O_3 and 2% FeP in the final refinements; the LaFePO is stoichiometric as indicated by the free refinement of the occupancies. The inset of Fig. 1(a) shows a comparison of the (220) reflection at $T=298$ and 10 K. There is no sign of peak broadening or splitting that would indicate a structural transition similar to that observed in LaFeAsO.[8,14] Furthermore, there is no observable difference in the residuals between $T=298$ and 10 K, implying a lack of long-range magnetic order. As an additional check for weak magnetic super-reflections, low angle, high count rate neutron-diffraction data were collected at $T=7$, 100, 200, and

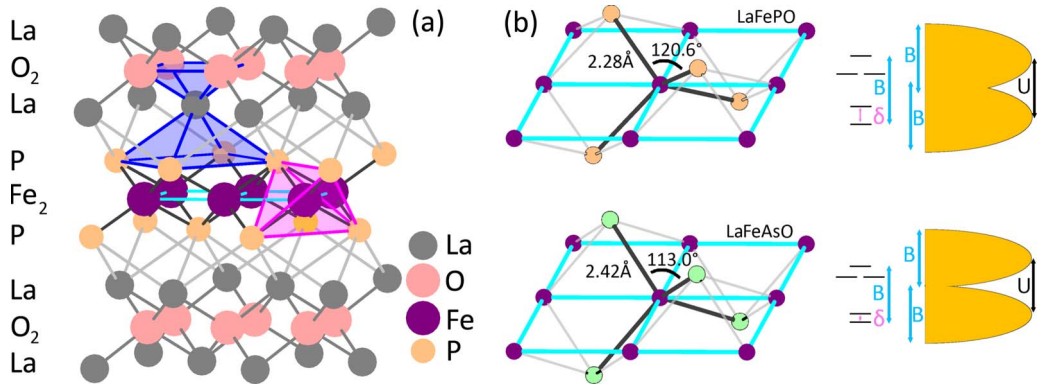

FIG. 2. (Color online) (a) The structure of tetragonal LaOFeP consists of alternating La-O_2-La and P-Fe_2-P layers. One iron pnictide tetrahedron is shaded, as are the planes forming a square antiprism coordination of a La^{3+} ion. Ionic sizes were used for La^{3+} and O^{2-} whereas covalent sizes were used for Fe and P. (b) Extracted portions of the iron-pnictide layer for LaFePO and LaFeAsO, showing both the square net of iron ions and the difference in the coordination tetrahedron in each case. Also shown is a simplified picture of how the less compressed tetrahedron in the arsenide case, which results in a smaller Jahn-Teller splitting (δ), would be expected to decrease the total bandwidth of the *d*-orbital-derived bands (b) and make the arsenide closer to localized, nonmetallic behavior.

TABLE I. Refined structural parameters at $T=298$ and 10 K. Space group P4/nmm (#129). Atomic positions: La: 2c (1/4,1/4,z), Fe: 2b (3/4,1/4,1/2), P: 2c (1/4,1/4,z), and O: 2a (3/4,1/4,0). In the first column, the formula was freely refined by fixing the occupancy of the iron site and letting all others vary. In the second column, the thermal parameters and overall scale factor were held fixed, and all occupancies were allowed to vary. The final refinements (columns 3 and 4) fixed all occupancies at unity. Anisotropic thermal parameters were used. The sample contained 0.7% La_2O_3 and 2% FeP. Lattice parameters are in units of angstrom and thermal parameters are in units of 10^{-2} Å^2.

	LaFePO	$T=298$ K (fixed iron n)	$T=298$ K (fixed U)	$T=298$ K (fixed n)	$T=10$ K (fixed n)
	a	3.96307(4)	3.96306(4)	3.96306(4)	3.95667(4)
	c	8.5087(1)	8.5087(1)	8.5087(1)	8.4973(1)
La	z	0.1488(2)	0.1488(2)	0.1487(2)	0.1493(2)
	$U_{11}=U_{22}$	0.84(6)	0.79	0.79(5)	0.31(4)
	U_{33}	0.57(9)	0.52	0.52(8)	0.28(8)
	n	1.02(1)	1.004(4)	1	1
Fe	$U_{11}=U_{22}$	0.69(5)	0.75	0.75(5)	0.32(4)
	U_{33}	0.75(8)	0.81	0.81(7)	0.28(7)
	n	1	0.995(4)	1	1
P	z	0.6348(3)	0.6347(3)	0.6348(3)	0.6354(3)
	$U_{11}=U_{22}$	0.8(1)	0.80	0.80(8)	0.56(7)
	U_{33}	0.7(1)	0.7	0.7(1)	0.2(1)
	n	1.01(1)	0.997(7)	1	1
O	$U_{11}=U_{22}$	0.80(9)	0.73	0.73(7)	0.58(6)
	U_{33}	0.9(1)	0.8	0.8(1)	0.4(1)
	n	1.02(1)	1.007(6)	1	1
	χ^2	1.197	1.195	1.198	1.470
	R_{wp}	6.19%	6.19%	6.20%	6.66%
	R_p	4.93%	4.93%	4.94%	4.98%
	$R(F^2)$	4.67%	4.73%	4.71%	4.64%

320 K. All observed peaks are indexed and well fitted by the nuclear structure of LaFePO. Thus we observe no long-range magnetic order in LaFePO. The detectability limit indicates that any ordered moment, if the magnetic structure is analogous to that in LaFeAsO,[14] would have to be less than $0.07\mu_B$/Fe. Thus we conclude that, above $T=10$ K, LaFePO shows no structural distortion or long-range magnetic ordering.

In addition to being metallic, the magnetic susceptibility (Fig. 3) data are essentially flat from $T=1.8-300$ K, showing contributions only from Pauli paramagnetism and Landau diamagnetism (corrections for core diamagnetism and the sample holder were applied). This is in contrast to an impure specimen containing traces of Fe_2P, which shows pronounced magnetic behavior. There is a slight upturn in the susceptibility of the pure sample between $T=200$ and 250 K that is attributable to the impurity FeP [Curie temperature 215 K (Ref. 35)], and a further small upturn below $T=20$ K that may be due to either a paramagnetic impurity or the proposed spin fluctuations (see below). However, these features are small and indicate the lack of magnetism in a pure sample. When combined with the neutron-diffraction data, which show the absence of long-range magnetic order (see above), this implies that LaFePO is nonmagnetic above $T=1.8$ K. For comparison to previous literature reports, we also show the dc susceptibility measured under a low field ($\mu_0 H=0.0005$ T) (top inset) as well as an ac measurement scaled per gram of sample (bottom inset). Both show negligible responses to the applied field with no downturn at low temperatures. The level of Fe_2P and FeP in this sample, indicated by the magnitude of the upturn around $T=200-250$ K (see above), is less than that observed in samples, which show a superconducting transition.[30] As such, the lack of superconductivity in our sample is not attributable to the presence of small amounts of either Fe_2P or FeP. Rather, this lack of downturn indicates that stoichiometric LaFePO is not superconducting above $T=1.8$ K.

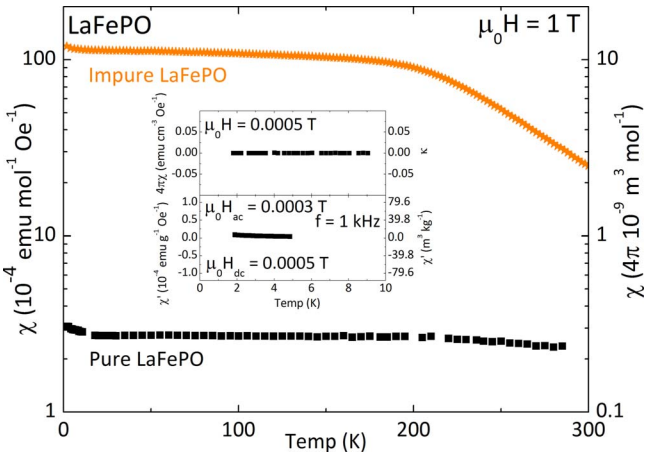

FIG. 3. (Color online) DC magnetization data at $\mu_0H=1$ T (main panel) and $\mu_0H=0.0005$ T (top inset) show that LaFePO is nonsuperconducting and nonmagnetic above 1.8 K. The dc magnetization on an impure sample containing 2% Fe_2P is also plotted. For comparison to the literature, the bottom inset shows an ac magnetization measurement of this sample, which shows no trace of superconductivity (the scale is ten times more sensitive than previous reports).[3,29,30]

To check for superconductivity at lower temperatures, resistivity measurements were done from $T=0.35-300$ K, as shown in Fig. 4(a). The data are normalized to the room-temperature value ($\rho_{300}=1.51$ mΩ cm) as the measured resistivity on a polycrystalline sample is often sensitive to grain-boundary and surface effects, and higher than the intrinsic values. The resistivity decreases to $\rho_{20}=0.61$ mΩ cm at $T=20$ K. Furthermore, the thermopower [Fig. 4(b)] is small and negative. Thus LaFePO is an *n*-type metal. Importantly, there is no downturn in the resistivity even at the lowest temperatures [left half of inset of Fig. 4(a)], indicating that the stoichiometric sample of LaFePO is not superconducting. However, the residual resistivity ratio (RRR) is 2.5, lower than that expected for a pure material free of defects and disorder, and there is a slight upturn in the resistivity below $T=20$ K to $\rho_{0.35}=0.64$ mΩ cm at $T=0.35$ K. The most likely origin for both of these observations is scattering at grain boundaries in the polycrystalline pellet. However, these results could also be intrinsic to LaFePO and the result of weak localization or other effects. One indication that the upturn may be intrinsic is our observation of a small but positive magnetoresistance under an applied field of $\mu_0H=9$ T [right half of inset of Fig. 4(a)] that is greatest at the resistivity minimum. Positive magnetoresistances are unusual and not readily explained solely by grain-boundary effects, and the fact that the magnetoresistance maximum occurs at the resistivity minimum suggests that the two are related. Furthermore, the thermopower data also show a minimum at a similar temperature and the magnetization (see above) has a slight upturn. High quality single crystals would be helpful in determining the origin of these results. The present data show that LaFePO is an *n*-type metal that is nonsuperconducting above $T=0.35$ K.

The nonmagnetic, metallic nature of LaFePO is confirmed by specific-heat measurements. Figure 5 shows the low-

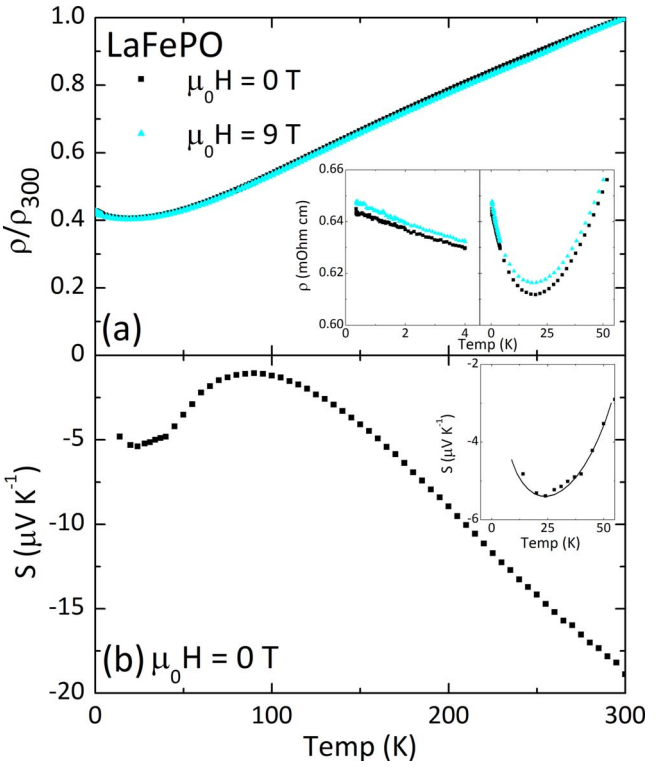

FIG. 4. (Color online) (a) Resistivity measurements on a polycrystalline pellet show that LaFePO is metallic and displays a slight positive magnetoresistance. The left inset shows the low-temperature region confirming the nonsuperconducting nature of this sample. The right inset shows the observed resistivity minimum, possibly from spin fluctuations. (b) Thermopower data show that LaFePO is an *n*-type metal. An upturn at low temperatures is also observed (inset).

temperature specific heat at $\mu_0H=0$, 1, 3, and 9 T. At all four fields there is a sharp upturn at the lowest temperatures ($T<1$ K). A plot of CT^2 versus T^3 below $T=1$ K (inset of Fig. 5) is linear for all four cases. Thus the sharp increase can be described as the high-temperature portion of a Schottky anomaly with a contribution to the specific heat of $C_{\text{shottky}}=\frac{B}{T^2}$. This term is ascribed to the freezing out of nuclear spins of either ^{31}P(S=1/2) and/or ^{139}La(S=7/2). The lack of a comparable upturn in the case of CeFePO,[36] and the presence of an upturn in the case of LaNiAsO,[37] suggests that the origin is ^{139}La. In addition to the Schottky anomaly, there is a broad upturn in the $\mu_0H=0$ T data that starts at higher temperatures ($T\approx5$ K). This broad upturn is weakly enhanced at $\mu_0H=1$ T and suppressed by $\mu_0H=9$ T. It is well described by a logarithmic contribution to the specific heat of $C_{\text{sf}}=AT^3$ ln T. Therefore the specific heat below $T=10$ K was fit to the formula $C=\gamma T+\beta T^3+AT^3$ ln T$+\frac{B}{T^2}$, where γ, β, A, and B are refinable parameters. The fits are quite good, as shown in Fig. 5, and the values of the parameters are given in Table II. The fitted Sommerfeld coefficients (γ) are very close to what is expected[38,42] from the predicted density of states at the Fermi level ($\gamma_{\text{calc}}=14.1\frac{\text{mJ}}{\text{mol K}^2}$), implying a negligible effective-mass enhancement. This is also consistent with the measured susceptibility (Fig. 3): $\chi_{\text{meas}}=3.1\times10^{-9}\frac{\text{m}^3}{\text{mol}}$ ($=2.4\times10^{-4}\frac{\text{emu}}{\text{mol Oe}}$) is close to the expected

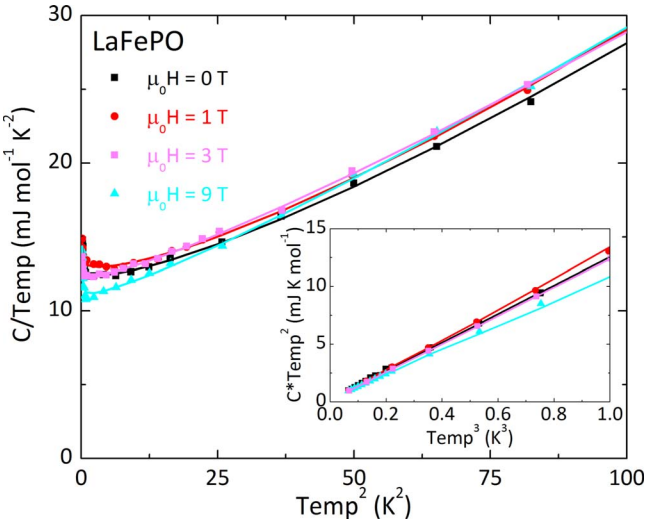

FIG. 5. (Color online) Specific-heat measurements show both a Schottky anomaly below 1 K and T^3 ln T behavior responsible for the broad upturn around 5 K. The lines are fits to the data (see text). The T^3 ln T contribution is suppressed under an applied field, suggesting that its origin is spin fluctuations. The inset shows a fit to the $T<1$ K data showing good agreement with a Schottky anomaly.

value,[43] $\chi_{\mathrm{calc}}=2.4\times10^{-9}\frac{\mathrm{m}^3}{\mathrm{mol}}$ $(=1.9\times10^{-4}\frac{\mathrm{emu}}{\mathrm{mol\ Oe}})$. Although it is impossible to separate the Pauli and Landau components of the measured susceptibility from our data, the Stoner enhancement factor, indicative of the degree of exchange enhancement in the system, can be estimated as $S=\frac{3}{2}\cdot\frac{\chi_{\mathrm{meas}}}{\chi_{\mathrm{calc}}}=1.9$, where the numerical prefactor converts the measured susceptibility to estimate the Pauli contribution.[44] This is small and, given the large predicted density of states at the Fermi level, would not be expected to cause an observable mass enhancement in γ. However, $S>1.0$ implies exchange-enhanced behavior and the presence of the logarithmic contribution to the specific heat is consistent with this picture. Taking the enhancement as arising from the presence of spin fluctuations (LaFePO is predicted to be near a magnetic instability), the spin-fluctuation temperature T_{sf} and lattice contribution β_3 can be extracted from the fitted β and A values.[45] The values obtained are $T_{\mathrm{sf}}=14.3$ K and $\beta_3=0.199\frac{\mathrm{mJ}}{\mathrm{mol\ K}^4}$. The small value of T_{sf} is consistent with the observed suppression of the logarithmic term under high fields and the concomitant decrease in γ. It is also consistent with the Stoner enhancement factor estimated from the susceptibility data: using this T_{sf}, the measured γ, and the fitted coefficient A at $\mu_0H=1$ T, the calculated[46] Stoner enhancement factor is $S=1.5$, in reasonable agreement with $S=1.9$ from the susceptibility data (especially given the number of assumptions). The value of β_3 corresponds to a Debye temperature of $\theta_D=340$ K, similar to what was found for LaNiAsO. Thus the specific-heat data of LaFePO are consistent with LaFePO, being a nonmagnetic metal with weak exchange enhancement from spin fluctuations. The origins of these fluctuations deserve further study, and could also explain the minimum in the resistivity and thermopower measurements.

IV. DISCUSSION

These results are substantially different than those for the related compound LaFeAsO. Recent research has shown that LaFeAsO is a metal that undergoes a structural distortion at $T=150$ K followed by the formation of a spin-density wave (SDW) at $T=134$ K.[8,14] We see no evidence for either kind of transition in LaFePO, down to $T=10$ K, by neutron diffraction. This might be qualitatively explained by the fact that the Fe-Fe separation is larger in LaFeAsO than it is in LaFePO (2.85 Å versus 2.80 Å), meaning that it should be closer to localized (magnetic) electron behavior. The Fe-Fe separation of undoped SmFeAsO is reported to be only 2.79 Å,[7] smaller than what we find for LaFePO, but SmFeAsO exhibits the same peak in the resistivity that is seen at the structural transition in LaFeAsO near $T=150$ K.[7] This suggests that the in-plane metal-metal distance is not the critical factor in driving the structural distortion. Instead, we propose that the important structural feature is the shape of the iron-pnictide tetrahedron. Figure 2(b) shows a comparison of the Fe-pnictide tetrahedron in LaFePO and LaFeAsO.[14] The Fe-X bond distance increases by 6%, from 2.28 Å (X=P) to 2.41 Å (X=As), a consequence of the larger size of As relative to P. This change (0.13 Å) is close to what is expected from related compounds (e.g., the mean Fe-X bond distance increases by 0.13 Å between FeP and FeAs). Although the bond lengths increase by 6%, the in-plane Fe-Fe distance only increases by 2%. This is consistent with the fact that the dimensions of the ionic La-O_2-La layer are expected to be fixed by the size of La^{3+} and O^{2-} ions. Since each lanthanum ion is also coordinated to four pnictide ions [Fig. 2(a)], the in-plane dimensions of the X-Fe_2-X layer will be primarily determined by the La-O_2-La network, which is consistent with what is observed. Thus when going from P to As, the larger size of the pnictide results in a substantial expansion of the c axis to obtain favorable Fe-As bond lengths. Thus the tetrahedron in LaFeAsO is less compressed than in LaFePO [Fig. 2(b)] with a top As-Fe-As bond

TABLE II. Parameters extracted from fits of the low-temperature specific heat of LaFePO.

Applied field	γ (mJ mol^{-1} K^{-2})	β (mJ mol^{-1} K^{-4})	A (mJ mol^{-1} K^{-4})	B (mJ K mol^{-1})
0 T	12.5(1)	−0.098(26)	0.111(12)	0.17(2)
1 T	13.1(1)	−0.117(20)	0.120(8)	0.13(2)
3 T	12.3(1)	0.0004(2)	0.072(4)	0.10(1)
9 T	11.0(1)	0.031(3)	0.066(1)	0.22(2)

angle of 113.0 ° compared to a P-Fe-P angle of 120.6 ° (an ideal tetrahedron would have an angle of 109.5 °). This decreases the Jahn-Teller splitting of the *d*-orbital-derived bands [Fig. 2(b)] and reduces the energy range spanned by *d*-derived states. In turn this means that intrasite electron correlations (Hubbard U) can drive the As system closer to localized, nonmetallic behavior. This qualitative chemical explanation matches recent theoretical work, which showed that LaFeAsO is close to opening a gap at the Fermi level due to electron-electron correlations.[39]

V. CONCLUSION

In conclusion, our dc and ac magnetization, resistivity, specific-heat, and neutron-diffraction data show that stoichiometric LaFePO is nonmagnetic and nonsuperconducting above $T=0.35$ K. These results suggest that the superconductivity observed in the LaFePO system may be due to either oxygen deficiency,[40] as has been reported in the case of LaFeAsO,[16] or the presence of superconducting impurities such as $LaFe_4P_{12}$ ($T_c=4.1$ K),[41] lanthanum metal ($T_c=6.9$ K), or tin flux inclusions ($T_c=3.1$ K). In contrast to LaFeAsO, which shows both a structural and SDW transition, we find that LaFePO is a normal metal with no magnetic behavior except a T^3 ln T contribution to the specific-heat data at low temperatures that is attributable to spin fluctuations. We propose that the differences in the shape of the metal-pnictide tetrahedron between the P and As cases, due to the size difference of the pnictide and chemical pressure of the La-O_2-La framework, are responsible for the radically different properties observed.

Note added in proof. Superconductivity at 38 K was recently reported[47] in K-doped $BaFe_2As_2$, which has the same iron-pnictide layers as in the LnOFeX family.

ACKNOWLEDGMENTS

T.M.M. gratefully acknowledges support by the National Science Foundation Graduate Research Program. The work at Princeton was supported by the Department of Energy, Division of Basic Energy Sciences, through Grant No. DE-FG02-98ER45706.

[1] B. I. Zimmer, W. Jeitschko, J. H. Albering, R. Glaum, and M. Reehuis, J. Alloys Compd. **229**, 238 (1995).
[2] P. Quebe, L. J. Terbuchte, and W. Jeitschko, J. Alloys Compd. **302**, 70 (2000).
[3] Y. Kamihara, H. Hiramatsu, M. Hirano, R. Kawamura, H. Yanagi, T. Kamiya, and H. Hosono, J. Am. Chem. Soc. **128**, 10012 (2006).
[4] Y. Qiu, M. Kofu, W. Bao, S. H. Lee, Q. Huang, T. Yildirim, J. R. D. Copley, J. W. Lynn, T. Wu, G. Wu, and X. H. Chen, arXiv:0805.1062 (unpublished).
[5] A. J. Drew, F. L. Pratt, T. Lancaster, S. J. Blundell, P. J. Baker, R. H. Liu, G. Wu, X. H. Chen, I. Watanabe, V. K. Malik, A. Dubroka, K. W. Kim, M. Roessle, and C. Bernhard, arXiv:0805.1042 (unpublished).
[6] Y. Nakai, K. Ishida, Y. Kamihara, M. Hirano, and H. Hosono, J. Phys. Soc. Jpn. **77**, 073701 (2008).
[7] L. Ding, C. He, J. K. Dong, T. Wu, R. H. Liu, X. H. Chen, and S. Y. Li, Phys. Rev. B **77**, 180510 (2008).
[8] T. Nomura, S. W. Kim, Y. Kamihara, M. Hirano, P. V. Sushko, K. Kato, M. Takata, A. L. Shluger, and H. Hosono, arXiv:0804.3569 (unpublished).
[9] C. Ren, Z. S. Wang, H. X. Yang, X. Zhu, L. Fang, G. Mu, L. Shan, and H. H. Wen, arXiv:0804.1726 (unpublished).
[10] B. Lorenz, K. Sasmal, R. P. Chaudhury, X. H. Chen, R. H. Liu, T. Wu, and C. W. Chu, arXiv:0804.1582 (unpublished).
[11] Z. W. Zhu, Z. A. Xu, X. Lin, G. H. Cao, C. M. Feng, G. F. Chen, Z. C. Li, J. L. Luo, and N. L. Wang, New J. Phys. **10**, 063021 (2008).
[12] G. Giovannetti, S. Kumar, and J. Brink, arXiv:0804.0866, J. Phys. B (to be published).
[13] P. Cheng, L. Fang, H. X. Yang, X. Zhu, G. Mu, H. Luo, Z. S. Wang, and H. H. Wen, Sci. China, Ser. G **51**, 719 (2008).
[14] C. Cruz, Q. Huang, J. W. Lynn, J. Q. Li, W. I. Ratcliff, J. L. Zarestky, H. A. Mook, G. F. Chen, J. L. Luo, N. L. Wang, and P. Dai, Nature (London) **453**, 899 (2008).
[15] H. W. Ou, J. F. Zhao, Y. Zhang, D. W. Shen, B. Zhou, L. X. Yang, C. He, F. Chen, M. Xu, T. Wu, X. H. Chen, Y. Chen, and D. L. Feng, Chin. Phys. Lett. **25**, 2225 (2008).
[16] Z. A. Ren, G. C. Che, X. L. Dong, J. Yang, W. Lu, W. Yi, X. L. Shen, Z. C. Li, L. L. Sun, F. Zhou, and Z. X. Zhao, arXiv:0804.2582 (unpublished).
[17] Z. A. Ren, W. Lu, J. Yang, W. Yi, X. L. Shen, Z. C. Li, G. C. Che, X. L. Dong, L. L. Sun, F. Zhou, and Z. X. Zhao, Chin. Phys. Lett. **25**, 2215 (2008).
[18] Z. A. Ren, J. Yang, W. Lu, W. Yi, G. C. Che, X. L. Dong, L. L. Sun, and Z. X. Zhao, arXiv:0803.4283 (unpublished).
[19] Z. A. Ren, J. Yang, W. Lu, W. Yi, X. L. Shen, Z. C. Li, G. C. Che, X. L. Dong, L. L. Sun, F. Zhou, and Z. X. Zhao, Europhys. Lett. **82**, 57002 (2008).
[20] G. F. Chen, Z. C. Li, G. Li, J. Zhou, D. Wu, J. Dong, W. Z. Hu, P. Zheng, Z. J. Chen, J. L. Luo, and N. L. Wang, arXiv:0803.0128, Phys. Rev. Lett. (to be published).
[21] G. F. Chen, Z. C. Li, D. Wu, J. Dong, G. Li, W. Z. Hu, P. Zheng, J. L. Luo, and N. L. Wang, Chin. Phys. Lett. **25**, 2235 (2008).
[22] G. F. Chen, Z. C. Li, D. Wu, G. Li, W. Z. Hu, J. Dong, P. Zheng, J. L. Luo, and N. L. Wang, Phys. Rev. Lett. **100**, 247002 (2008).
[23] L. Shan, Y. Wang, X. Zhu, G. Mu, L. Fang, and H. H. Wen, arXiv:0803.2405 (unpublished).
[24] X. Zhu, H. X. Yang, L. Fang, G. Mu, and H. H. Wen, arXiv:0803.1288(unpublished).
[25] T. Y. Chen, Z. Tesanovic, R. H. Liu, X. H. Chen, and C. L. Chien, Nature (London) **453**, 1224 (2008).
[26] X. H. Chen, T. Wu, G. Wu, R. H. Liu, H. Chen, and D. F. Fang, Nature (London) **453**, 761 (2008).
[27] F. Hunte, J. Jaroszynski, A. Gurevich, D. C. Larbalestier, R. Jin, A. S. Sefat, M. A. McGuire, B. C. Sales, D. K. Christen, and D. Mandrus, Nature (London) **453**, 903 (2008).
[28] Y. Kamihara, T. Watanabe, M. Hirano, and H. Hosono, J. Am.

Chem. Soc. **130**, 3296 (2008).
[29] C. Y. Liang, R. C. Che, H. X. Yang, H. F. Tian, R. J. Xiao, J. B. Lu, R. Li, and J. Q. Li, Supercond. Sci. Technol. **20**, 687 2007).
[30] M. Tegel, I. Schellenberg, R. Poettgen, and D. Johrendt, arXiv:0805.1208 (unpublished).
[31] J. P. Carlo, Y. J. Uemura, T. Goko, G. J. MacDougall, J. A. Rodriguez, W. Yu, G. M. Luke, P. Dai, N. Shannon, S. Miyasaka, S. Suzuki, S. Tajima, G. F. Chen, W. Z. Hu, J. L. Luo, and N. L. Wang, arXiv:0805.2186 (unpublished).
[32] Y. Kamihara, M. Hirano, H. Yanagi, T. Kamiya, Y. Saitoh, E. Ikenaga, K. Kobayashi, and H. Hosono, Phys. Rev. B **77**, 214515 (2008).
[33] B. H. Toby, J. Appl. Crystallogr. **34**, 210 (2001).
[34] A. C. Larson and R. B. Von Dreele, Los Alamos National Laboratory Report No. LAUR 86, 2000 (unpublished).
[35] M. E. Schlesinger, Chem. Rev. (Washington, D.C.) **102**, 4267 (2002).
[36] E. M. Bruening, C. Krellner, M. Baenitz, A. Jesche, F. Steglich, and C. Geibel, arXiv:0804.3250 (unpublished).
[37] Z. C. Li, G. F. Chen, J. Dong, G. Li, W. Z. Hu, D. Wu, S. K. Su, P. Zheng, T. Xiang, N. L. Wang, and J. L. Luo, arXiv:0803.2572 (unpublished).
[38] S. Lebegue, Phys. Rev. B **75**, 035110 (2007).
[39] K. Haule, J. H. Skim, and G. Kotliar, Phys. Rev. Lett. **100**, 226402 (2008).
[40] R. C. Che, R. J. Xiao, C. Y. Liang, H. X. Yang, C. Ma, H. Shi, and J. Q. Li, Phys. Rev. B **77**, 184518 (2008).
[41] G. P. Meisner, Physica B & C **108**, 763 (1981).
[42] $g(\varepsilon_F)_{\text{calc}}=6\frac{\text{states}}{\text{eV cell}}$ so $\gamma_{\text{calc}}=g(\varepsilon_F)_{\text{calc}}/424.25=14.1\frac{\text{mJ}}{\text{mol K}^2}$.
[43] $\chi_{\text{calc}}=\mu_B^2 g(\varepsilon_F)_{\text{calc}}=2.4\times10^{-9}\frac{\text{m}^3}{\text{mol}}$.
[44] $\chi_{\text{meas}}=\chi_{\text{pauli}}+\chi_{\text{landau}}\approx\chi_{\text{pauli}}-\frac{1}{3}\chi_{\text{pauli}}=\frac{2}{3}\chi_{\text{pauli}}$, where the relation $\chi_{\text{landau}}=-\frac{1}{3}\chi_{\text{pauli}}$, assuming a free-electron gas, has been used.
[45] For spin fluctuations, $\beta=\beta_3-A\ \ln T_{sf}$ and thus a plot of β versus A will be linear with intercept β_3 and slope $-\ln T_{sf}$.
[46] For spin fluctuations, $A=\frac{\alpha\gamma_0}{T_{sf}^2}$, where γ_0 does not include any mass enhancement from the spin fluctuations and $\alpha=\frac{6\pi^2}{5}\frac{(S-1)^2}{S}$. For a system with negligible mass enhancement, $\gamma_0=\gamma_{\text{meas}}$.
[47] M. Rotter, M. Tegel, and D. Johrendt, arXiv:0805.4630 (unpublished).